Supporting Information

Anion Transport with Pnictogen Bonds in Direct Comparison with Chalcogen and Halogen Bonds

Lucia M. Lee, Maria Tsemperouli, Amalia I. Poblador-Bahamonde, Sebastian Benz, Naomi Sakai, Kaori Sugihara,* and Stefan Matile*

School of Chemistry and Biochemistry, NCCR Chemical Biology, University of Geneva, Geneva, CH-1211 Geneva, Switzerland

stefan.matile@unige.ch, kaori.sugihara@unige.ch

Table of Content

1. Materials and Methods

As in reference S1, Supporting Information. Reagents for synthesis of carriers were purchased from Merck, Apollo Scientific and Acros. Carrier **6** was purchased from Sigma Aldrich and used without further purification.

Buffer solutions were prepared using salts of the analytical grade from Merck and Acros Organics. Fluorophores, 8-hydroxy-1,3,6-pyrenetrisulfonate and (5)6-carboxyfluorescein were obtained from Merck, egg yolk phosphatidylcholine (EYPC), egg yolk phosphatidylglycerol (EYPG), 1-palmitoyl-2-oleoyl-*sn*-glycero-3-phosphocholine (POPC) and a Mini-Extruder used for vesicle preparation were purchased from Avanti Polar Lipids. Fluorescence measurements were performed with a FluoroMax-4 spectrofluorometer from Horiba Scientific equipped with a stirrer and a temperature controller. Fluorescence spectra were corrected using instrument-supplied correction factors, unless stated otherwise. All measurements were performed at 25 °C. ^{19}F NMR spectra were recorded on a Bruker 300 MHz spectrometer.

Abbreviations. BLM: Black lipid membranes; CF: 5(6)-Carboxyfluorescein; DMSO: Dimethyl sulfoxide; EYPC: Egg yolk phosphatidylcholine; EYPG: Egg yolk phosphotidylglycerol; FCCP: Carbonyl cyanide 4-(trifluoromethoxy) phenylhydrazone; HEPES: *N*-(2-Hydroxyethyl)piperazine-*N'*-(2-ethanesulfonic acid); HPTS: 8-Hydroxy-1,3,6-pyrenetrisulfonate; LUVs: Large unilamellar vesicles; POPC: 1-Palmitoyl-2-oleoyl-*sn*-glycero-3-phosphocholine; rt: Room temperature; TBA: tetrabutylammonium; THF: Tetrahydrofuran.

2. Transporters

Transporters **1-4** and **7** were prepared and characterized following the previously reported procedures.[S1-S3]

3. Anion Binding

The binding constants were obtained by a reported NMR titration method.[S1] Stock solutions of carriers **4** (1.86 mM) and **6** (3.12 mM) were prepared in dry THF, and used to prepare solutions of TBAX (X= Br, I, NO_3, 12 mM). Various volumes of stock solution with or without TBAX were mixed in an NMR tube to reach the desired final TBAX concentration. ^{19}F NMR spectra were recorded with each addition. Differences in chemical shift $\Delta\delta$ of the most responsive fluorine signal, in *para* position to the hetero atom, were plotted versus TBAX concentration, and curve-fitted to a 1:1 binding isotherm to determine the dissociation constants according to equation (S1):

$$\Delta\delta = (\Delta\delta_{max} / [C]_0) \times (0.5 \times [A] + 0.5 \times [C]_0 + K_D) - (0.5 \times (([A^2) + (2 \times [A]) \times (K_D - [C]_0)) + (K_D + [C]_0)^2)^{0.5})) \tag{S1}$$

where $\Delta\delta = |\delta - \Delta\delta_0|$, [A] = concentration of TBAX (X= Br, I), and $[C]_0$ = concentration of carriers **4** and **6**.

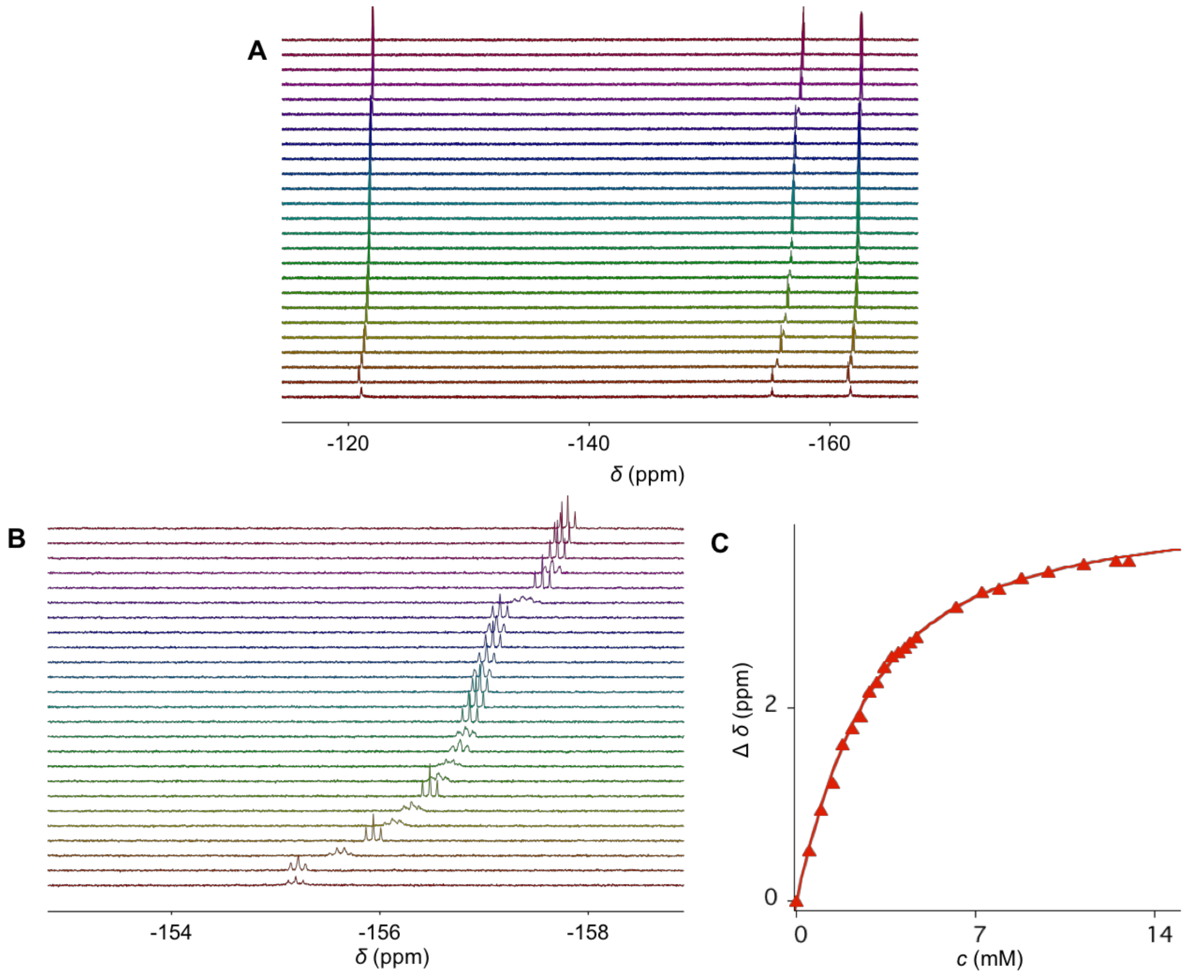

Figure S1. [19]F NMR spectra of (A, B) a solution of carrier **4** (1.86 mM) in THF with increasing concentration of TBABr (0 – 12.0 mM, bottom to top) and (C) nonlinear fitting of equation (S1) of changes in chemical shift $\Delta\delta$ versus TBABr concentration. $K_D = 1.71 \pm 0.05$ mM, $\delta_{max} = 4.10 \pm 0.03$ ppm, $R = 0.999$.

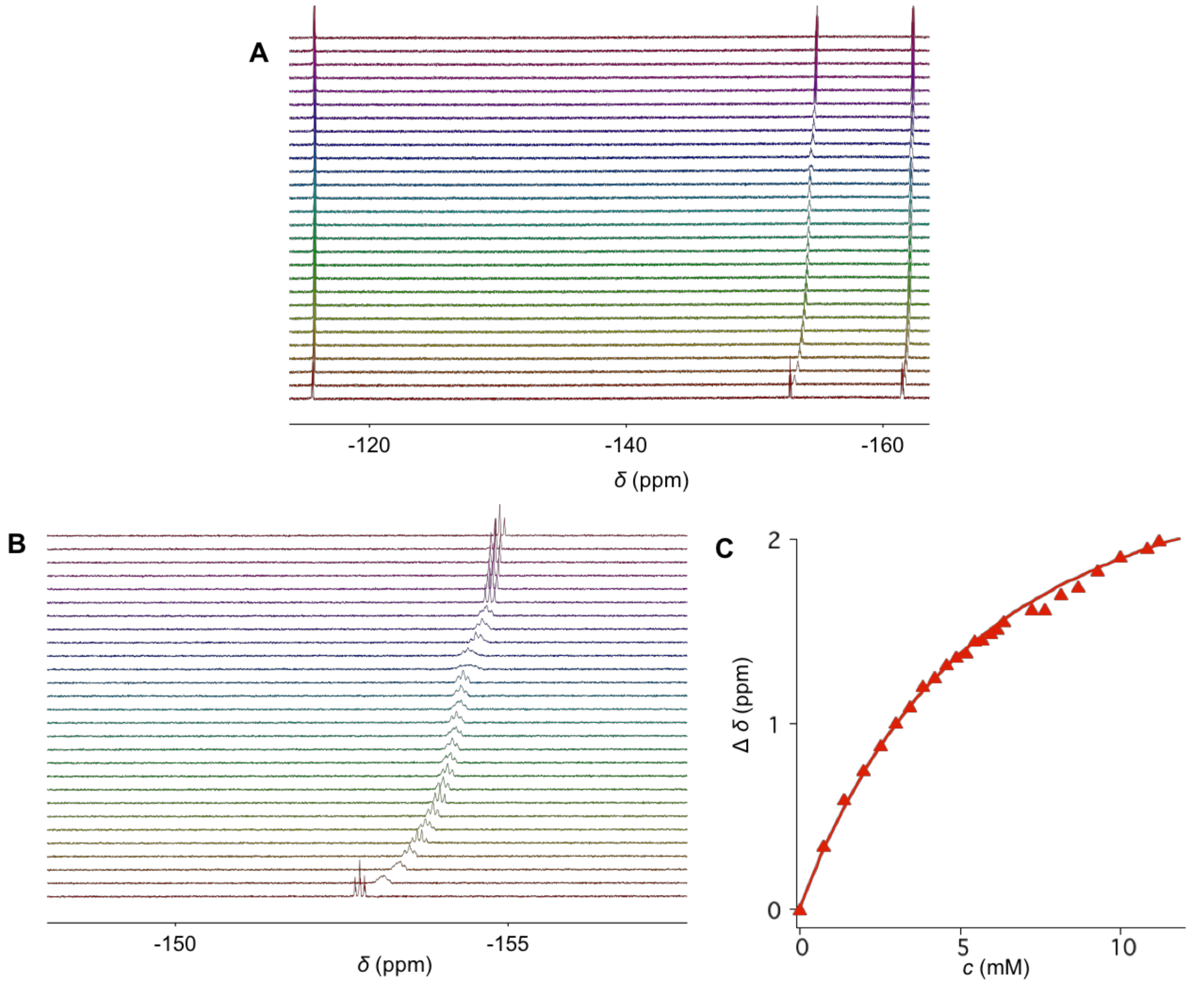

Figure S2. [19]F NMR spectra of (A) a solution of carrier **4** (1.86 mM) in THF with increasing concentration of TBAI (0 – 12.0 mM, bottom to top) and (B) nonlinear fitting of equation (S1), of changes in chemical shift $\Delta\delta$ versus TBAI concentration. $K_D = 4.31 \pm 0.18$ mM, $\delta_{max} = 2.82 \pm 0.04$ ppm, $R = 0.999$.

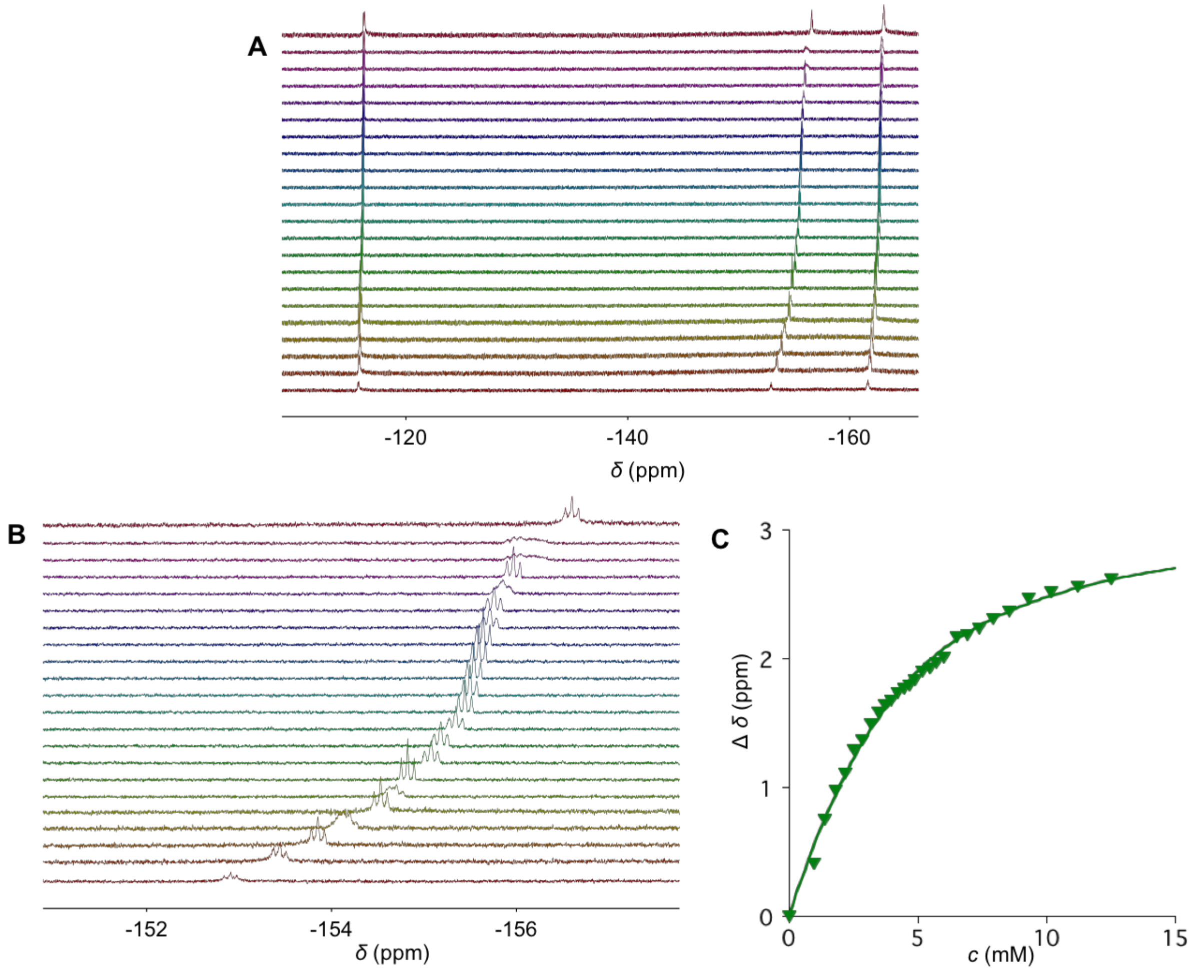

Figure S3. [19]F NMR spectra of (A) a solution of carrier **6** (3.12 mM) in THF with increasing concentration of TBABr (0 – 12.0 mM, bottom to top) and (B) nonlinear fitting of equation (S1), of changes in chemical shift $\Delta\delta$ versus TBABr concentration. $K_D = 2.02 \pm 0.14$ mM, $\delta_{max} = 3.13 \pm 0.06$ ppm, $R = 0.998$.

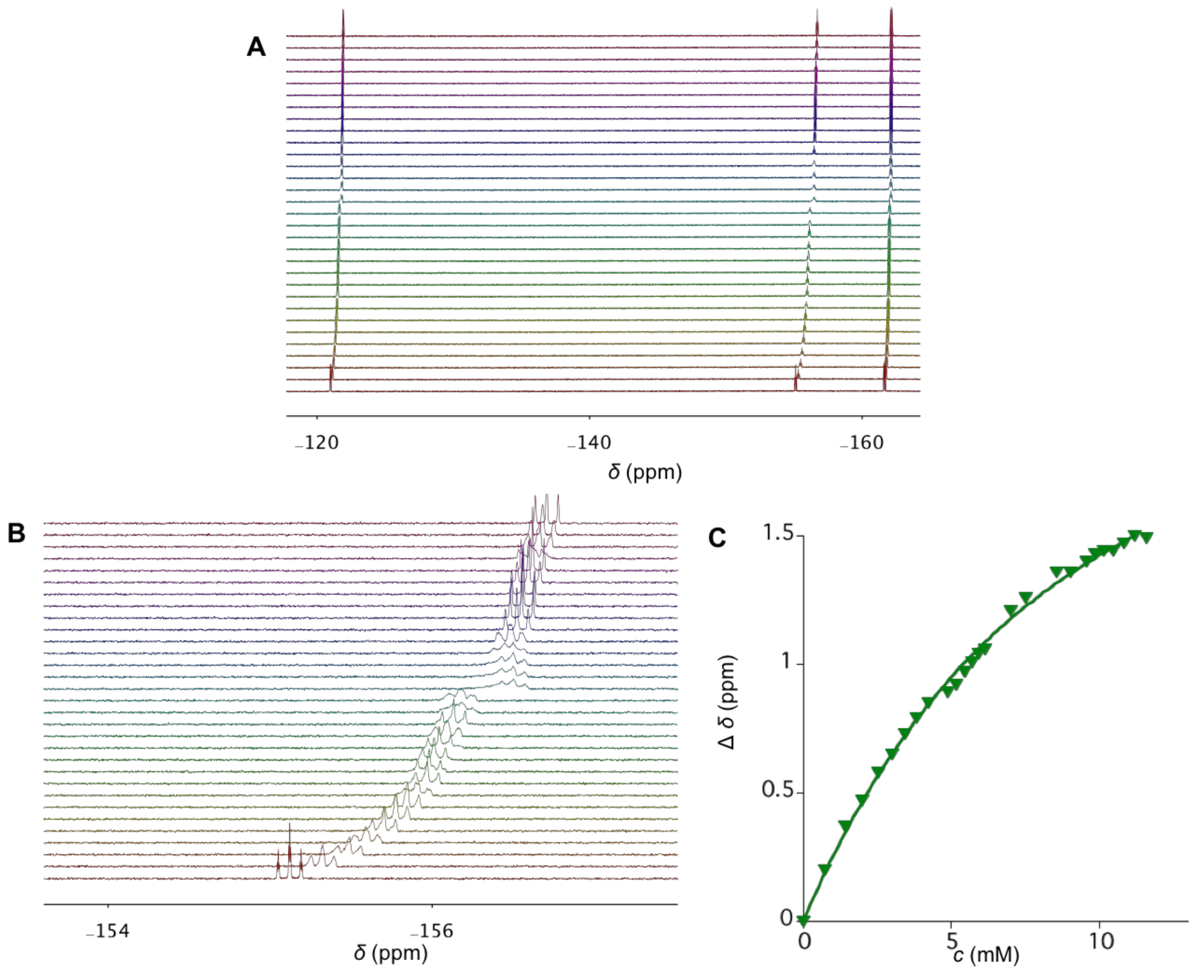

Figure S4. ^{19}F NMR spectra of (A) a solution of carrier **6** (3.12 mM) in THF with increasing concentration of TBAI (0 – 12.0 mM, bottom to top) and (B) nonlinear fitting of equation (S1), of changes in chemical shift $\Delta\delta$ versus TBAI concentration. $K_D = 6.32 \pm 0.36$ mM, $\delta_{max} = 2.51 \pm 0.06$ ppm, $R = 0.999$.

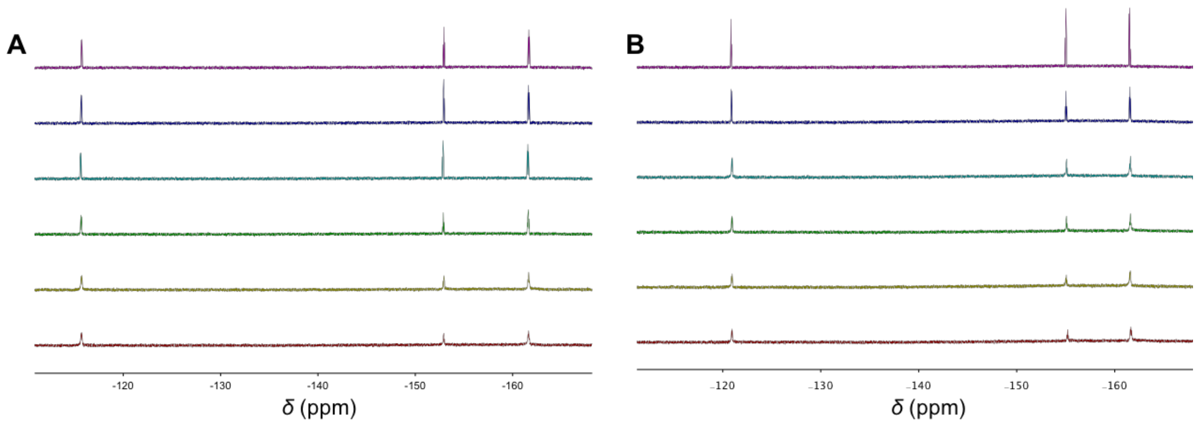

Figure S5. [19]F NMR spectra of carriers (A) **4** (1.86 mM) and (B) **6** (3.12 mM) with increasing concentration of $TBANO_3$ (0 – 12 mM, bottom to top). No significant shifts were observed up to a concentration of 12.0 mM of $TBANO_3$.

4. Anion Transport

4.1. Vesicle Preparation

EYPC-LUVs⊃HPTS. The procedure was followed as reported in the literature.[S4] A solution of EYPC (25 mg) in EtOH (25 µL) was diluted in $MeOH/CHCl_3$ (1:1, 2 mL). A thin lipid film was obtained by drying on a rotary evaporator (40 °C) and then *in vacuo* for 3 days. After hydration (>30 min) with 1.0 mL buffer (10 mM HEPES, 100 mM NaCl, 1.0 mM HPTS, pH 7.0), the resulting suspension was subjected to >5 freeze-thaw cycles (liquid N_2, 37 °C water bath) and >15 times extruded through a polycarbonate membrane (pore size 100 nm). Extravesicular components were removed by size exclusion chromatography (Sephadex G-50, Sigma-Aldrich) with 10 mM HEPES, 100 mM NaCl, pH 7.0. Final conditions: 5 mM EYPC, inside 10 mM HEPES, 100 mM NaCl, 1.0 mM HPTS, pH 7.0, outside: 10 mM HEPES, 100 mM NaCl, pH 7.0. The vesicles were used within the week of preparation.

EYPC/EYPG-LUVs⊃HPTS. These vesicles were prepared following the procedure described above using a mixture of EYPC and EYPG (9:1).

POPC-LUVs⊃CF. A thin film was prepared by evaporating a solution of POPC (25 mg) in MeOH/$CHCl_3$ (1:1, 2 mL) on a rotary evaporator (40 °C) and then *in vacuo* for 3 days.[S2] The film was then hydrated with 1.0 mL buffer (10 mM HEPES, 10 mM NaCl, 50 mM CF, pH 7.4), subjected to >5 freeze-thaw cycles (liquid N_2, 37 °C water bath) and >15 times extruded through a polycarbonate membrane (pore size 100 nm). Extravesicular components were removed by size exclusion chromatography (Sephadex G-50, Sigma-Aldrich) with 10 mM HEPES, 107 mM NaCl, pH 7.4. Final conditions: 5 mM POPC, inside 10 mM HEPES, 10 mM NaCl, 50 mM CF, pH 7.4, outside: 10 mM HEPES, 107 mM NaCl, pH 7.4. The vesicles were used within the week of preparation.

4.2. Ion Transport Activity

Following established procedures,[S4-S6] to a gently stirred, thermostated buffer (1950 µL, 25 °C, 10 mM HEPES, 100 mM NaX, X = Cl, Br or NO_3, or 10 mM HEPES, 95 mM NaI, 5 mM $Na_2S_2O_3$, pH 7.0) in a disposable plastic cuvette, EYPC (or EYPC/EYPG)-LUVs⊃HPTS (50 µL) was added. The time-dependent change in fluorescence intensity (λ_{em}= 510 nm) was monitored at two excitation wavelengths simultaneously ($I_{t,454}$: λ_{ex}= 454 nm, $I_{t,404}$: λ_{ex}= 404 nm), during addition of base (20 µL, 0.5 M NaOH) at t = 0.5 min, carrier (20 µL, THF solution) at t = 1.5 min, and gramicidin D (20 µL, 100 µM in DMSO) at t = 6 min.

Time course of fluorescence intensity I_t were obtained first by ratiometric analysis (R_t = $I_{t,454}$ / $I_{t,404}$), followed by normalization according to equation (S2),

$$I_{\mathrm{rel}} = \frac{(R_t - R_0)}{(R_\infty - R_0)} \qquad \text{(S2)}$$

where $R_0 = R_t$ at t = 1.5 min, before addition of carrier and $R_\infty = R_t$ at t = 8 min after addition of gramicidin D. I_{rel} at 6.5 min just before addition of gramicidin D was defined as transmembrane activity Y, and analyzed with the Hill equation (S3) to give effective concentration EC_{50} and the Hill coefficient n,

$$Y = Y_{\infty} + \frac{Y_0 - Y_{\infty}}{(1 + \frac{c}{EC_{50}})^n} \tag{S3}$$

where Y_0 is Y in absence of carrier, Y_{∞} is Y with excess carrier, and c is the carrier concentration in a cuvette. Complete results for all compounds are shown in Table 1.

4.3. FCCP Assay

A solution of EYPC-LUVs⊃HPTS (50 μL) was added to a gently stirred, thermostated (25 °C) buffer (1950 μL, 25 °C, 10 mM HEPES, 100 mM NaX, X = Cl, Br or NO_3, or 10 mM HEPES, 95 mM NaI, 5 mM $Na_2S_2O_3$, pH 7.0) in a disposable plastic cuvette.[S5] To this solution, the base (20 μL, 0.5 M NaOH) was added at t = 0.5 min, followed by FCCP (20 μL, 0.1 mM in DMSO) at t = 0.9 min, carrier (20 μL, THF solution) at t = 1.9 min, and gramicidin D (20 μL, 100 μM in DMSO) at t = 6 min. Data were obtained and analyzed as described in the section 4.2.

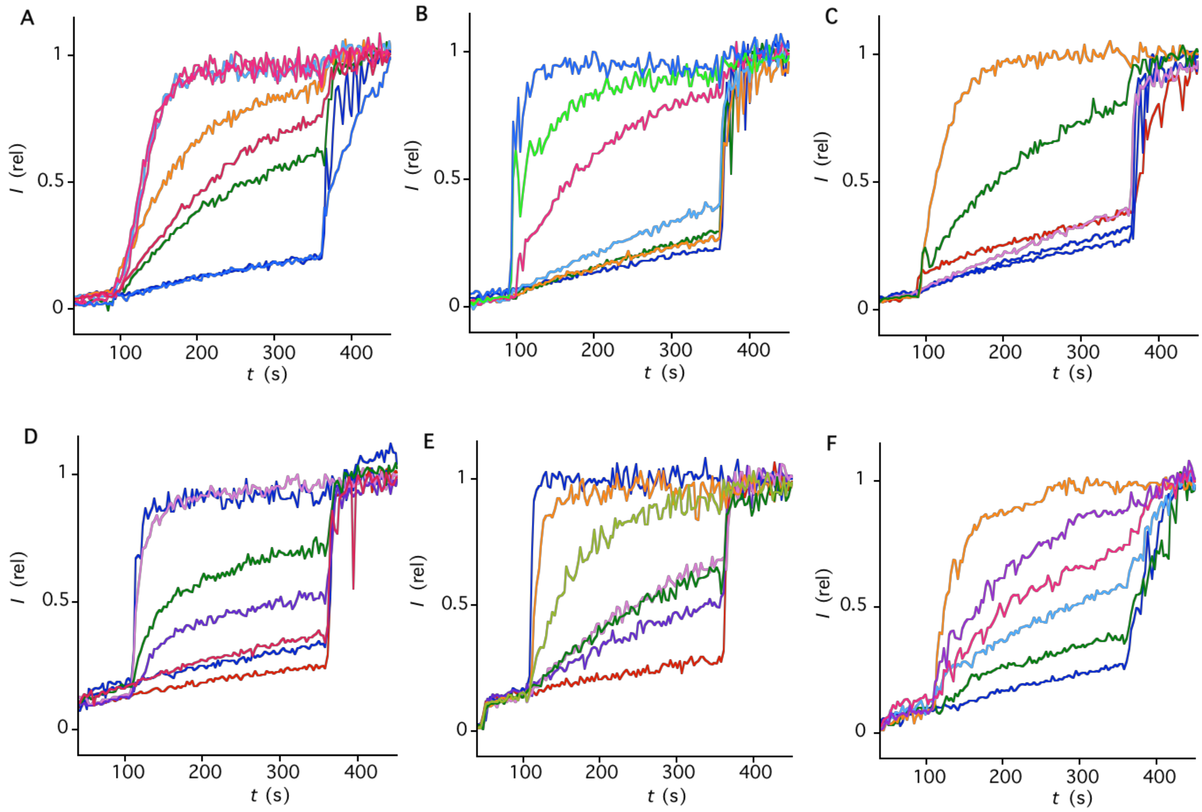

Figure S6. Fluorescence traces for compounds **2**, **4**, and **6** in the HPTS assay (**A-C** respectively) and the FCCP assays (**D-F** respectively) in EYPC-LUVs⊃HPTS in a NaCl buffer at different carrier concentrations. (A) Fractional emission I_{rel} during the addition of NaOH (5 mM, 30 s), **2** (concentration in cuvette with increasing activity: 0, 0.1, 1, 1.5, 2, 4, 6 and 10 µM, 90 s) and gramicidin D (1.0 µM, 360 s) to EYPC-LUVs⊃HPTS in a NaCl buffer (10 mM HEPES, 100 mM NaCl, pH 7.0). (B) Same for **4** (0, 0.04, 0.06, 0.1, 0.4, 0.8 and 4 µM). (C) Same for **6** (0, 40, 100, 150, 400 µM, and 1 mM). (D) Fractional emission I_{rel} during the addition of NaOH (5 mM, 30 s), FCCP (1.0 µM, 50 s), **2** (0, 0.004, 0.01, 0.03, 0.08, 0.4 and 1 µM, 90 s) and gramicidin D (1.0 µM, 360 s) to EYPC-LUVs⊃HPTS in a NaCl buffer (10 mM HEPES, 100 mM NaCl, pH 7.0). (E) Same for **4** (0, 0.009, 0.02, 0.03, 0.4, 2 and 8 µM). (F) Same for **6** (0, 40, 60, 100, 200 and 400 µM).

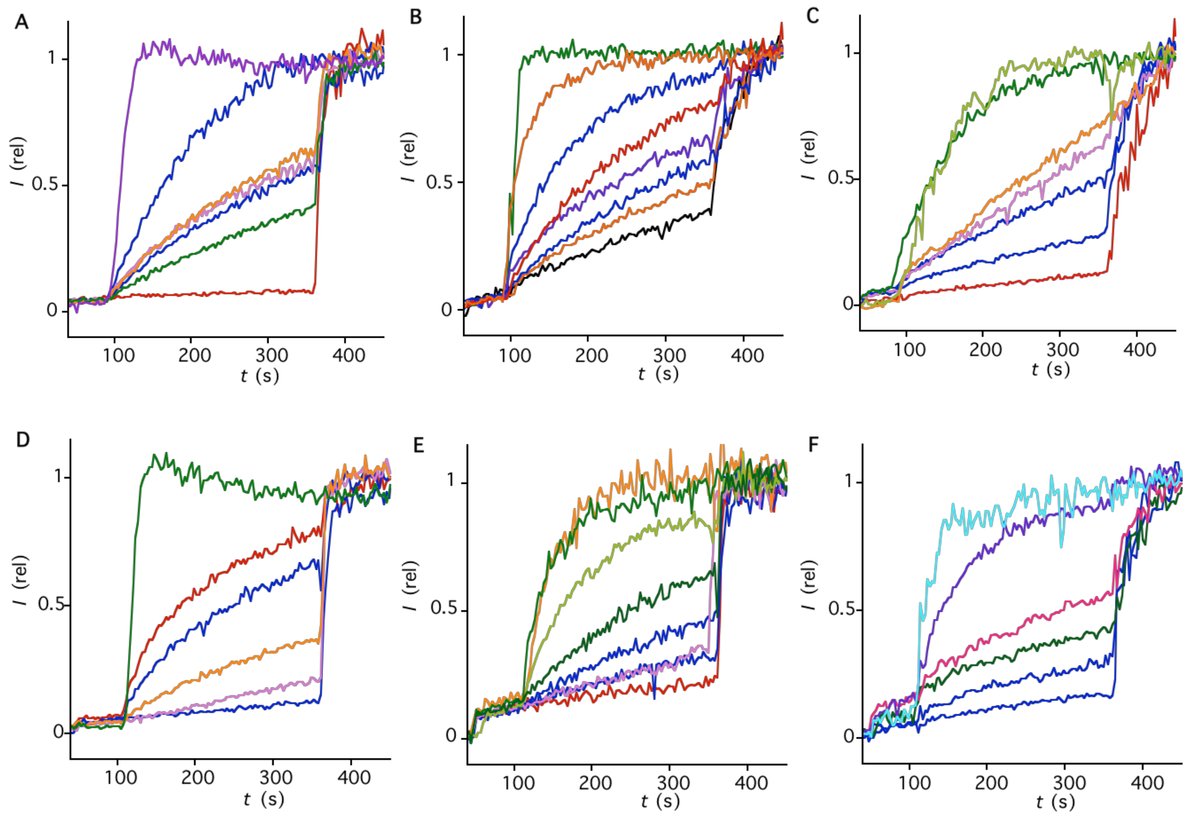

Figure S7. Fluorescence traces for compounds **2**, **4**, and **6** in the HPTS assay (**A**-**C** respectively) and the FCCP assays (**D**-**F** respectively) in EYPC-LUVs⊃HPTS in a $NaNO_3$ buffer at different carrier concentrations. (A) Fractional emission I_{rel} during the addition of NaOH (5 mM, 30 s), **2** (concentration in cuvette with increasing activity: 0, 0.4, 1, 2, 3, 15, and 80 µM, 90 s) and gramicidin D (1.0 µM, 360 s) to EYPC-LUVs⊃HPTS in a $NaNO_3$ buffer (10 mM HEPES, 100 mM $NaNO_3$, pH 7.0). (B) Same for **4** (0, 0.1, 0.4, 0.6, 0.8, 0.9, 1, and 10 µM). (C) Same for **6** (0, 9, 250, 400, 800 µM, 2.5 and 4 mM). (D) Fractional emission I_{rel} during the addition of NaOH (5 mM, 30 s), FCCP (1.0 µM, 50 s), **2** (0, 0.04, 0.1, 0.3, 0.6 and 4 µM, 90 s) and gramicidin D (1.0 µM, 360 s) to EYPC-LUVs⊃HPTS in a $NaNO_3$ buffer (10 mM HEPES, 100 mM $NaNO_3$, pH 7.0). (E) Same for **4** (0, 0.004, 0.008, 0.02, 0.05, 0.2, 0.4, and 1 µM) . (F) Same for **6** (0, 20, 40, 80 µM, 2 and 5 mM).

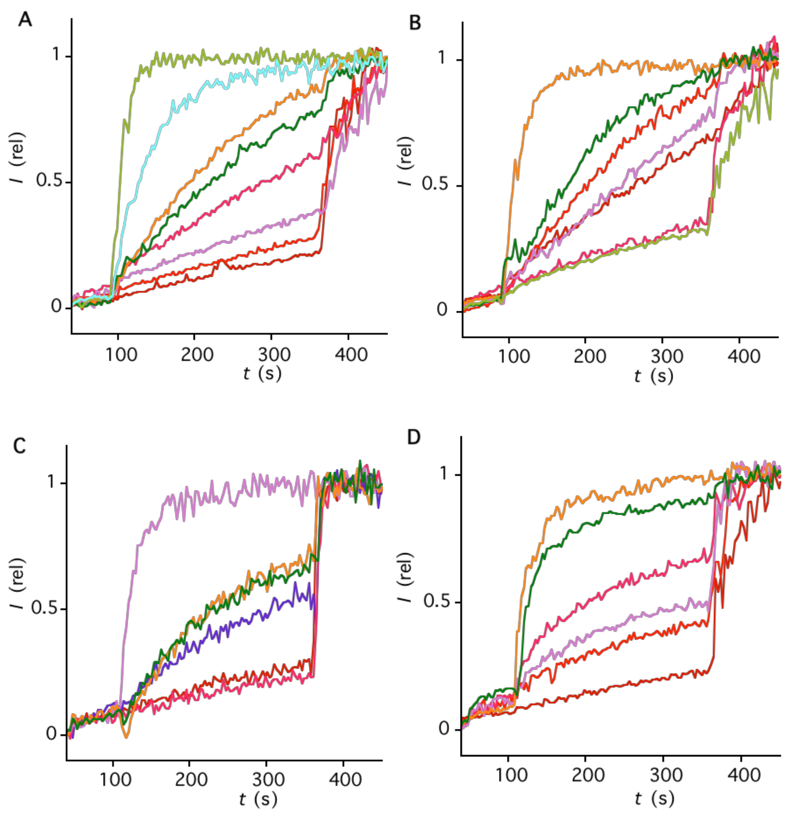

Figure S8. Fluorescence traces for compounds **4**, and **6** in the HPTS assay (**A**, **B** respectively) and the FCCP assays (**D**, F respectively) in EYPC-LUVs⊃HPTS in a NaBr buffer at different carrier concentrations. (A) Fractional emission I_{rel} during the addition of NaOH (5 mM, 30 s), **4** (concentration in cuvette with increasing activity: 0, 0.1, 0.2, 0.4, 0.6, 0.8, 2 and 4 µM, 90 s) and gramicidin D (1.0 µM, 360 s) to EYPC-LUVs⊃HPTS in a NaBr buffer (10 mM HEPES, 100 mM NaBr, pH 7.0). (B) Same for **6** (0, 80, 250, 300, 400, 800 µM, and 1 mM). (C) Fractional emission I_{rel} during the addition of NaOH (5 mM, 30 s), FCCP (1.0 µM, 50 s), **4** (0, 0.001, 0.02, 0.03, 0.04 and 2 µM, 90 s) and gramicidin D (1.0 µM, 360 s) to EYPC-LUVs⊃HPTS in a NaBr buffer (10 mM HEPES, 100 mM NaBr, pH 7.0). (D) Same for **6** (0, 0.8, 80, 100, 500, 800 µM).

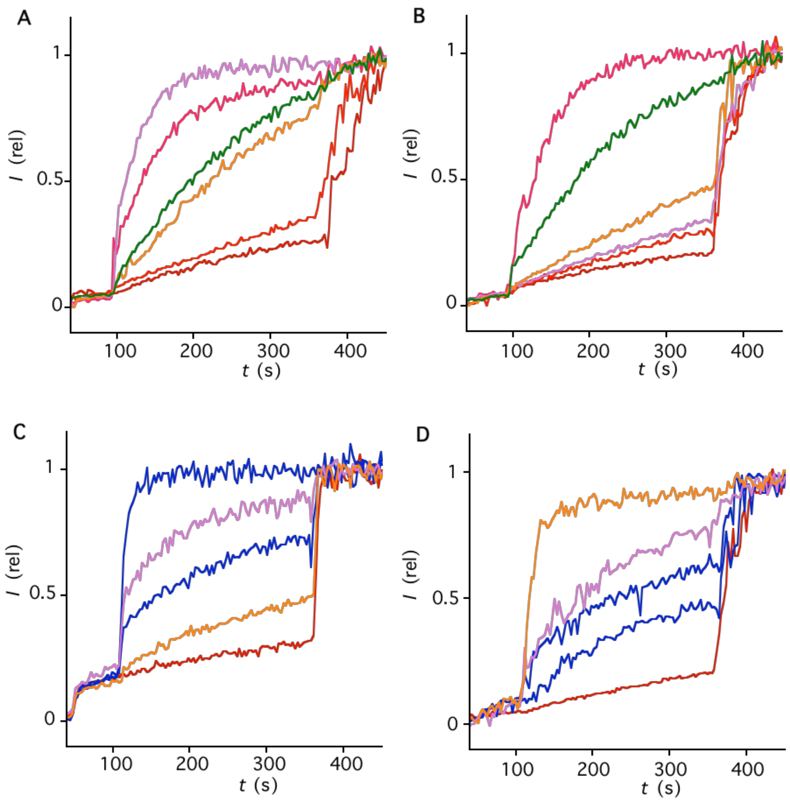

Figure S9. Fluorescence traces for compounds **4**, and **6** in the HPTS assay (**A-C** respectively) and the FCCP assays (**D-F** respectively) in EYPC-LUVs⊃HPTS in a NaI buffer at different carrier concentrations. (A) Fractional emission I_{rel} during the addition of NaOH (5 mM, 30 s), **4** (concentration in cuvette with increasing activity: 0, 0.08, 0.9, 1, 2, and 4 μM, 90 s) and gramicidin D (1.0 μM, 360 s) to EYPC-LUVs⊃HPTS in a NaI buffer (10 mM HEPES, 95 mM NaI, 5 mM $Na_2S_2O_3$, pH 7.0). (B) Same for **6** (0, 80, 100, 300, 500, and 800 μM). (C) Fractional emission I_{rel} during the addition of NaOH (5 mM, 30 s), FCCP (1.0 μM, 50 s), **4** (0, 0.008, 0.04, 0.08, and 4 μM, 90 s) and gramicidin D (1.0 μM, 360 s) to EYPC-LUVs⊃HPTS in a NaI buffer (10 mM HEPES, 100 mM NaI, pH 7.0). (D) Same for **6** (0, 200, 400, 600, and 800 μM).

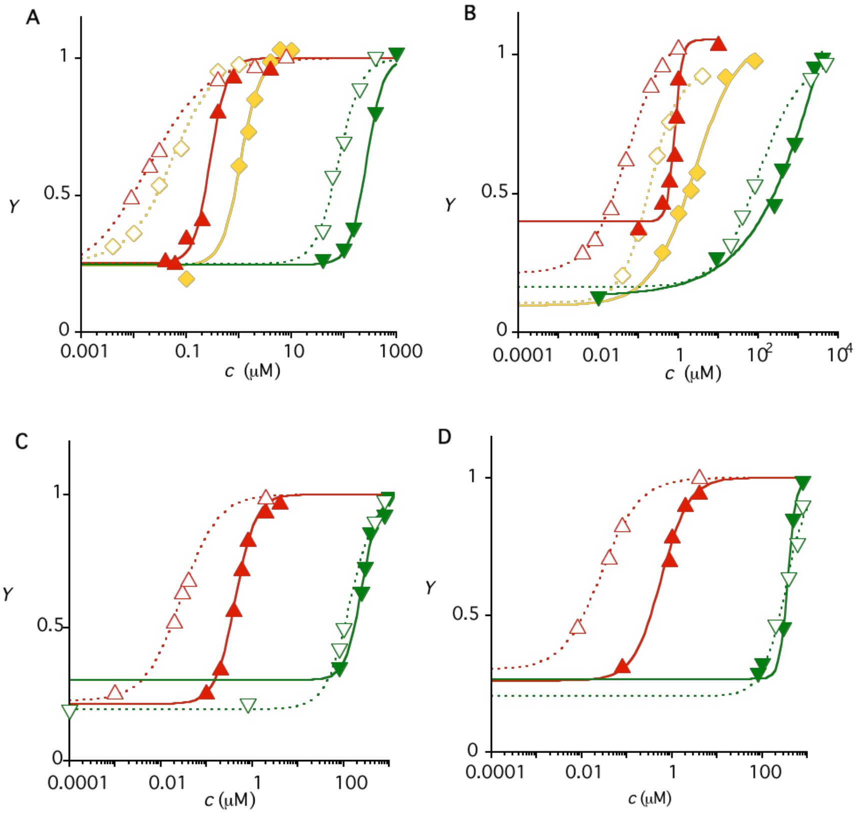

Figure S10. Combined dose response curves for carriers **2** (◆◇), **4** (▲△) and **6** (▼▽) in the HPTS (solid) and FCCP (dotted) assays in EYPC-LUVs⊃HPTS suspended in (A) a NaCl (10 mM HEPES, 100 mM NaCl, pH 7.0), (B) a $NaNO_3$ (10 mM HEPES, 100 mM $NaNO_3$, pH 7.0), (C) a NaBr (10 mM HEPES, 100 mM NaBr, pH 7.0), and (D) a NaI (10 mM HEPES, 95 mM NaI, 5 mM $Na_2S_2O_3$, pH 7.0) buffer.

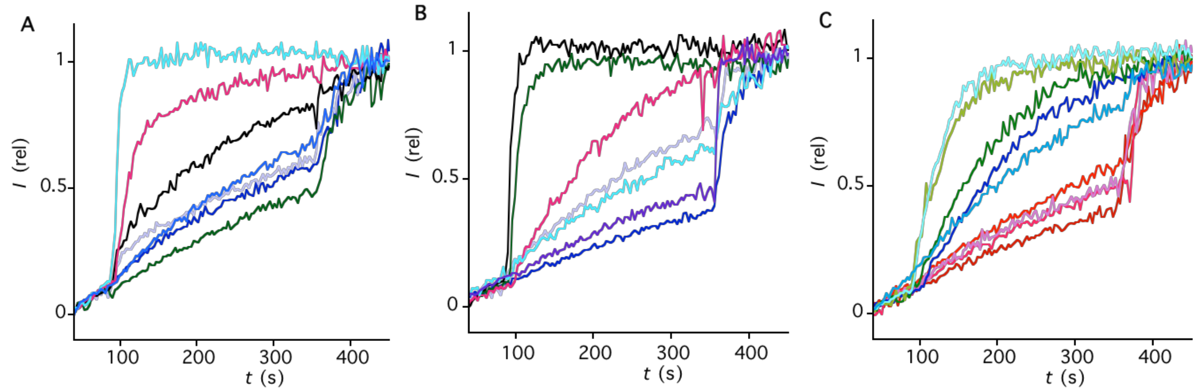

Figure S11. Fluorescence traces for carriers **2**, **4**, and **6** in the HPTS assay (**A**-**C** respectively) in anionic EYPG (10%) vesicles at different carrier concentrations. (A) Fractional emission I_{rel} during the addition of NaOH (5 mM, 30 s), **2** (concentration in cuvette with increasing activity: 0, 0.1, 1, 4, 10, 50, and 100 μM, 90 s) and gramicidin D (1.0 μM, 360 s) to EYPG/EYPC-LUVs⊃HPTS in a NaCl buffer (10 mM HEPES, 100 mM NaCl, pH 7.0). (B) Same for **4** (0, 0.02, 0.8, 1, 4, 10, and 100 μM). (C) Same for **6** (0, 100, 400, 500, 600, 700, 800, 900 μM, and 1 mM).

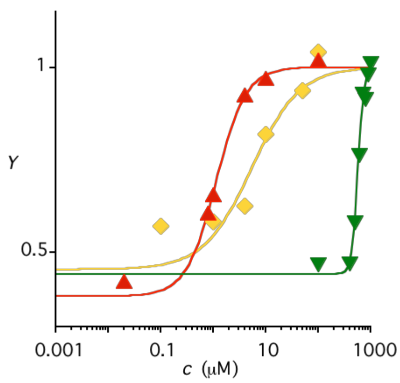

Figure S12. Dose response curves for carriers **2** (◆), **4** (▲) and **6** (▼) in the HPTS assay in 10% anionic EYPG vesicles as a function of carrier concentration.

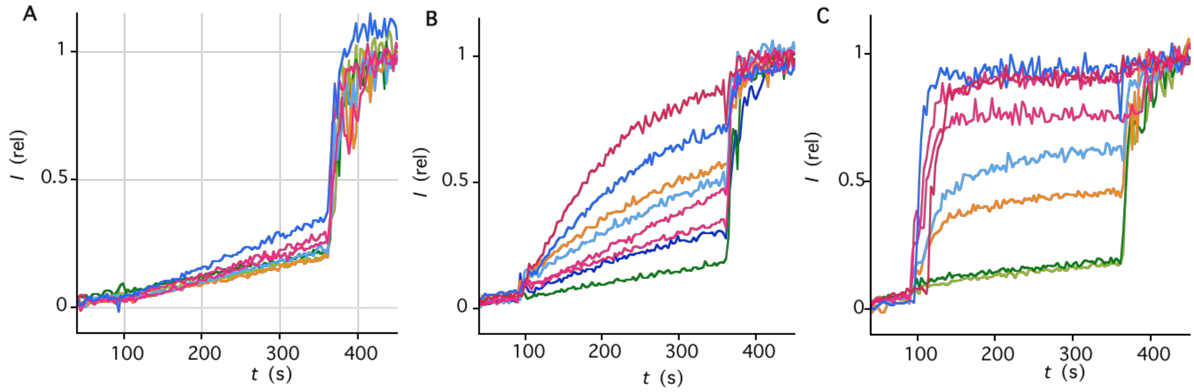

Figure S13. Fluorescence traces for compounds **1**, **3**, and **7** in the HPTS assay (**A-C** respectively) in EYPC-LUVs⊃HPTS in a NaCl buffer at different carrier concentrations. (A) Fractional emission I_{rel} during the addition of NaOH (5 mM, 30 s), **1** (concentration in cuvette with increasing activity: 0, 0.4, 0.8, 8, 20, 80, and 400 µM, 90 s) and gramicidin D (1.0 µM, 360 s) to EYPC-LUVs⊃HPTS in a NaCl buffer (10 mM HEPES, 100 mM NaCl, pH 7.0). (B) Same for **3** (0, 0.1, 0.4, 0.8, 1, 10, 40 and 80 µM). (C) Same for **7** (0, 0.8, 2, 4, 8, 40, 80, and 400 µM).

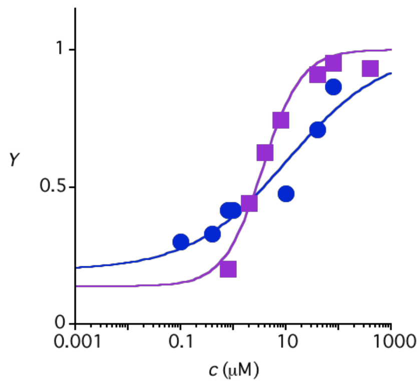

Figure S14. Combined dose response curves for carriers **3** (●) and **7** (■) in the HPTS assay in EYPC-LUVs⊃HPTS suspended in a NaCl buffer (10 mM HEPES, 100 mM NaCl, pH 7.0).

4.4. Non-Specific Leakage

To gently stirred, thermostated buffer (1950 µL, 25 °C, 10 mM HEPES, 107 mM NaCl, pH 7.4) in a disposable plastic cuvette, POPC-LUV⊃CF (50 µL) were added.[S6] The time-dependent changes in fluorescence intensity (I_t, λ_{ex}= 492 nm, λ_{em}= 517 nm) were monitored during the addition of the carrier at 100 s, and the addition of triton X-100 (40 µL, 1.2 % aq) at $t = 400$ s. Time courses of I_t were normalized to fractional intensities I_{rel} using equation (S2).

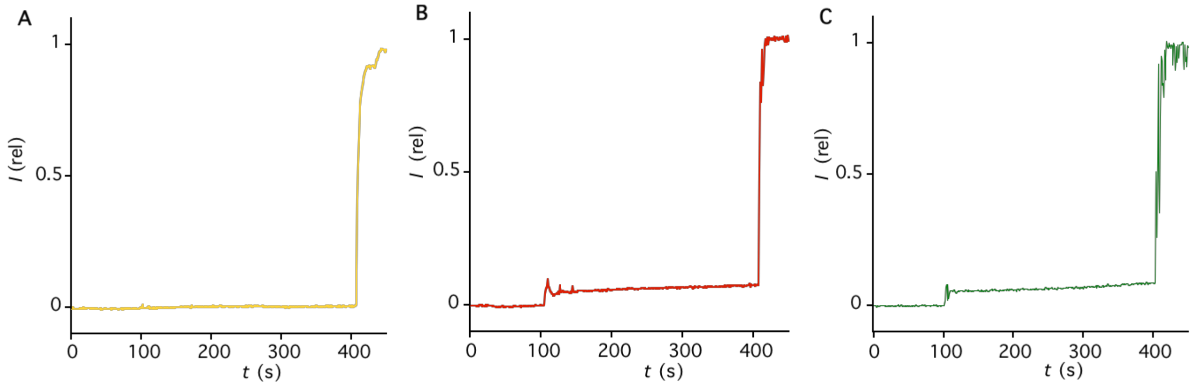

Figure S15. Change in emission intensity I_{rel} (λ_{ex}= 492 nm, λ_{em}= 517 nm) with time during the addition of **2** (10 mM, A), **4** (1 mM, B) and **6** (10 mM, C) and excess triton X-100 to EYPC vesicles with internal, self-quenched 5(6)-carboxyfluorescein (CF).

5. Planar Bilayer Conductance Experiment

Conductance experiments were performed in black lipid membranes as previously described.[S6] Briefly, black lipid membranes (BLMs) were prepared by painting a solution of POPC (25 mg/mL) in decane : hexane mixture (1 : 1 volume ratio) on a Teflon sheet with an aperture of a diameter d = 50 µm and a thickness l = 25 µm, mounted on a home-made electrochemical chamber.[S6] The Teflon sheet is separating two compartments *cis* and *trans*, where each of them contains 2 M NaCl (10 mM HEPES, pH 7.4). A Ag/AgCl electrode was connected to each chamber through an agar salt bridge (2M NaCl, 2% Agar). All the electrical measurements were performed with an Autolab PGSTAT302N potentiostat equipped with a FRA32 M module and ECD Module for low current recordings and Nova 1.11 software (Metrohm Ltd, Switzerland). The results were plotted with Igor Pro 7 analysis software (Wavemetrics, USA). The transporters were added to the *cis* compartment at negative holding potentials (*trans* side as ground), whereas the final concentration was 200, 300, 460, 500 and

100 μM for the carriers **4**, **6**, **7**, **1** and **2**, respectively. To determine ion selectivities of transporter **6**, **4** and **2**, transmembrane currents (*I*) were measured at different applied voltages (*V*) under asymmetric ionic conditions between the *cis* and *trans* compartments. Next the mean value of the current *I* response was plotted as a function of the applied voltages *V* and the reversal potentials (V_r) (which correspond to zero current voltages) were estimated after fitting the resulted *I-V* curves with a polynomial function. Chloride *vs* sodium permeability ratios P_{Cl^-} / P_{Na^+} were calculated from the reversal potentials (V_r) obtained under varied NaCl concentration gradients by using the Goldman-Hodgkin-Katz (GHK) equation (S4),[S9]

$$V_r = \frac{R \cdot T}{F} \ln \frac{P_{Na^+} \cdot [Na^+]_{trans} + P_{Cl^-} \cdot [Cl^-]_{cis}}{P_{Na^+} \cdot [Na^+]_{cis} + P_{Cl^-} \cdot [Cl^-]_{trans}} \quad \text{(S4)}$$

where P_{Na^+} and P_{Cl^-} are the ion permeabilities of sodium and chloride ions, V_r is the reversal potential, *F* the Faraday constant, *R* the gas constant and *T* the temperature in Kelvin. Next, anion selectivities were determined by measuring the reversal potentials upon exchange of the buffered NaCl solution in *trans* compartment with NaX (where X^- is NO_3^-, ClO_4^-, SO_4^{2-}). X anion *vs* chloride permeability ratios P_{X^-} / P_{Cl^-} were then calculated by using the equation derived from the following GHK equation (S5),

$$P_{X^-} / P_{Cl^-} = \frac{[Cl^-]_{cis}}{[X^-]_{trans} exp\left(\frac{V_r \cdot F}{R \cdot T}\right)} \quad \text{(S5)}$$

Formal gating charges were determined from *I-V* profiles using the equation (S6)

$$I = g_0 \cdot e^{\left(\frac{z_g \cdot e \cdot V}{k \cdot T}\right)} \quad \text{(S6)}$$

where *I* is the current (pA), z_g is the gating charge, *e* is the elemental charge, *V* is the applied voltage (V), *k* is the Boltzmann constant and *T* is the temperature in Kelvin.

All the values of reversal potentials, calculated permeabilities ratios and gating charges of carriers **6**, **4** and **2** are summarized in Table S1.

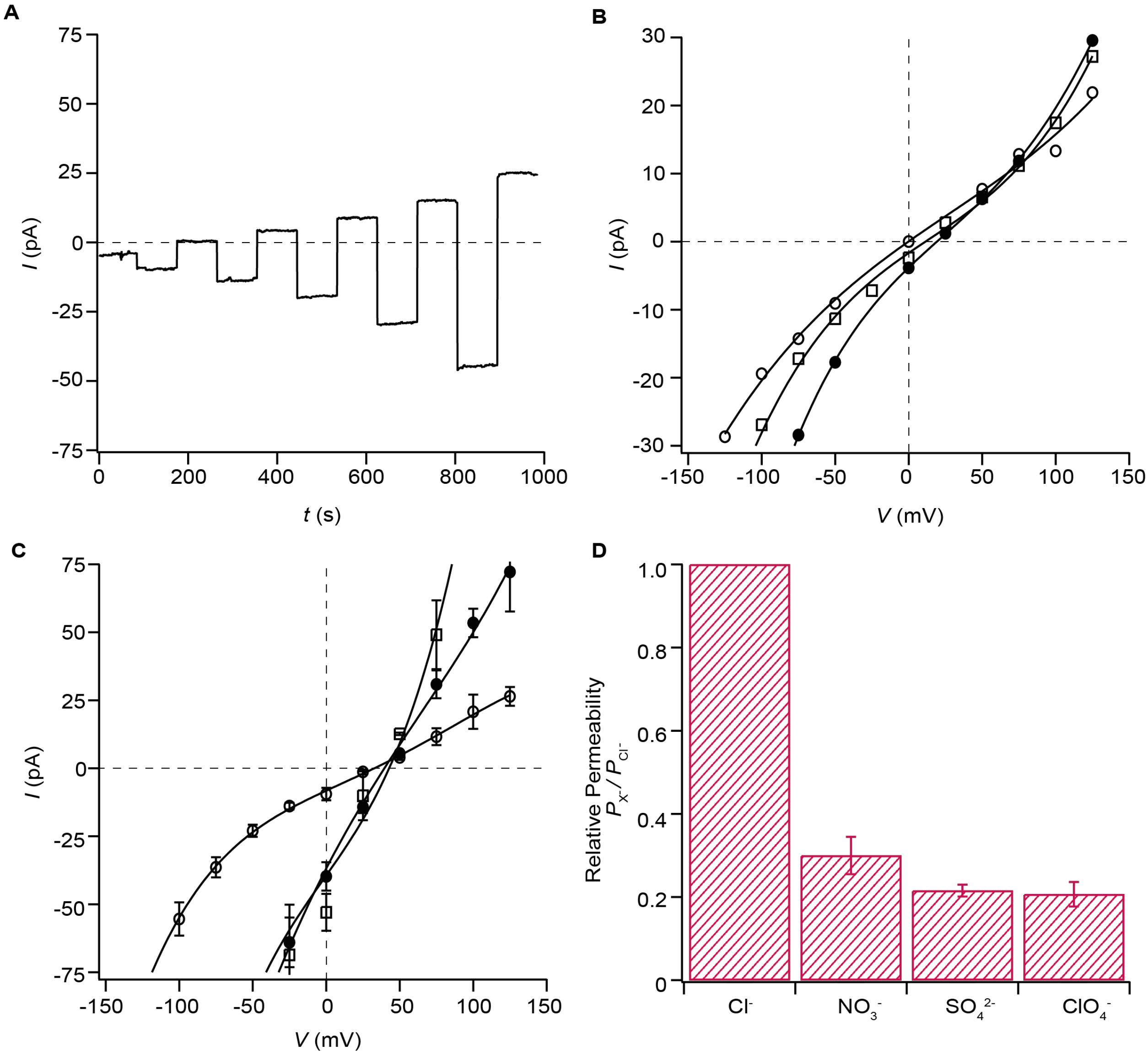

Figure S16. Ion transport characteristics of **6** studied in planar conductance measurements. (A) Current of **6** with 2 M NaCl *cis* and 1 M NaCl *trans* and $V(t)$ = 0 (0), -25 (90), +25 (180), -50 (240), +50 (380), -75 (420), +75 (500), -100 (600), +100 (700), -125 (800), +125 mV (900 s). (B) *I-V* profile of **6** with 2 M NaCl *cis* and 2 M (○), 1 M (□) or 0.5 M NaCl *trans* (●). (C) Same with 2 M $NaNO_3$ (○), 2 M $NaClO_4$ (□) or 1 M Na_2SO_4 *trans* (●). (D) Relative ion permeability of **6** normalized by the largest value of the observed ion permeability.

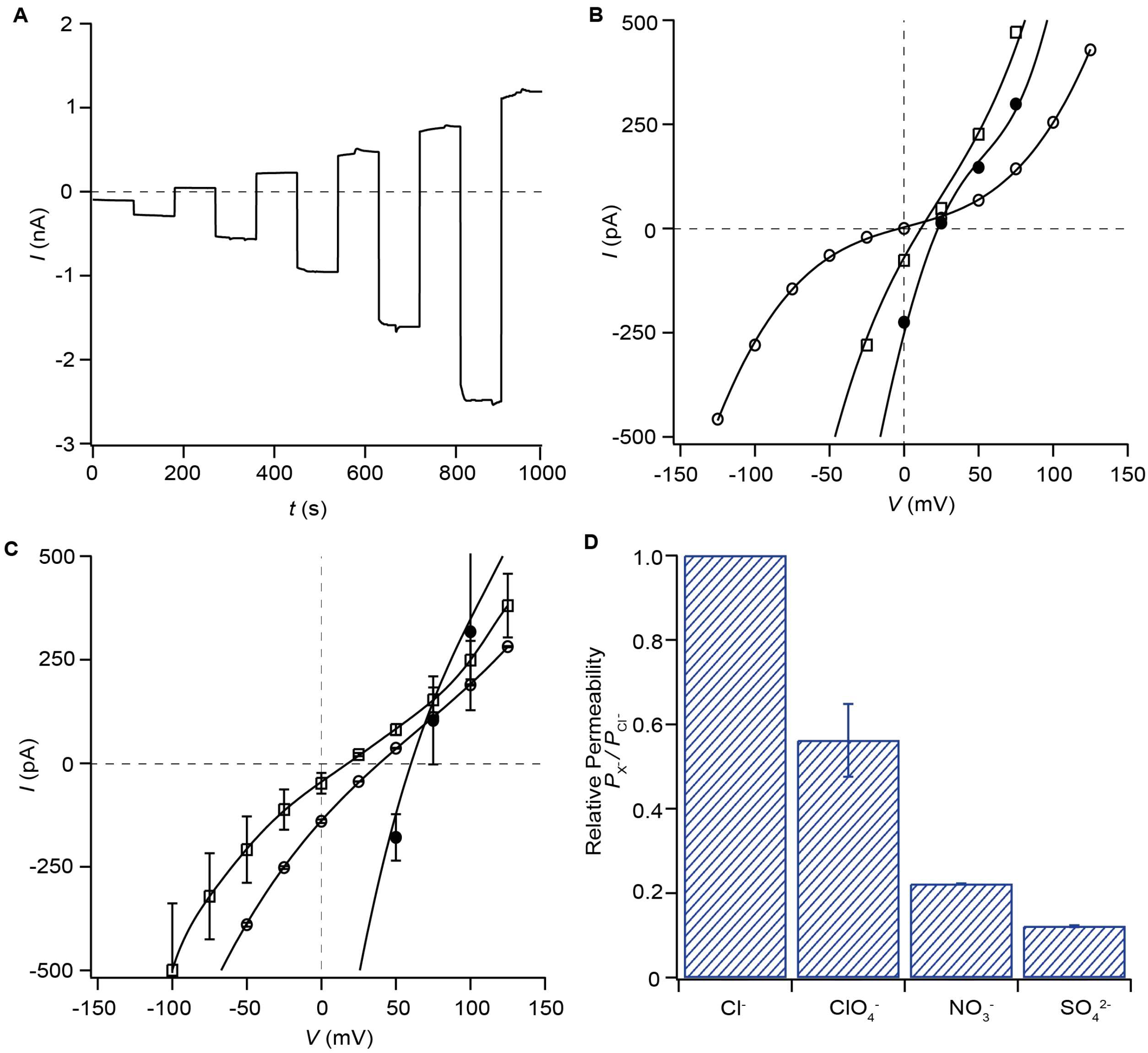

Figure S17. Ion transport characteristics of **4** studied in planar conductance measurements. (A) Current of **4** with 2 M NaCl *cis* and 1 M NaCl *trans* and $V(t)$ = 0 (0), -25 (90), +25 (180), -50 (240), +50 (380), -75 (420), +75 (500), -100 (600), +100 (700), -125 (800), +125 mV (900 s). (B) *I-V* profile of **4** with 2 M NaCl *cis* and 2 M (○), 1 M (□) or 0.5 M NaCl *trans* (●). (C) Same with 2 M $NaNO_3$ (○), 2 M $NaClO_4$ (□) or 1 M Na_2SO_4 *trans* (●). (D) Relative ion permeability of **4** normalized by the largest value of the observed ion permeability.

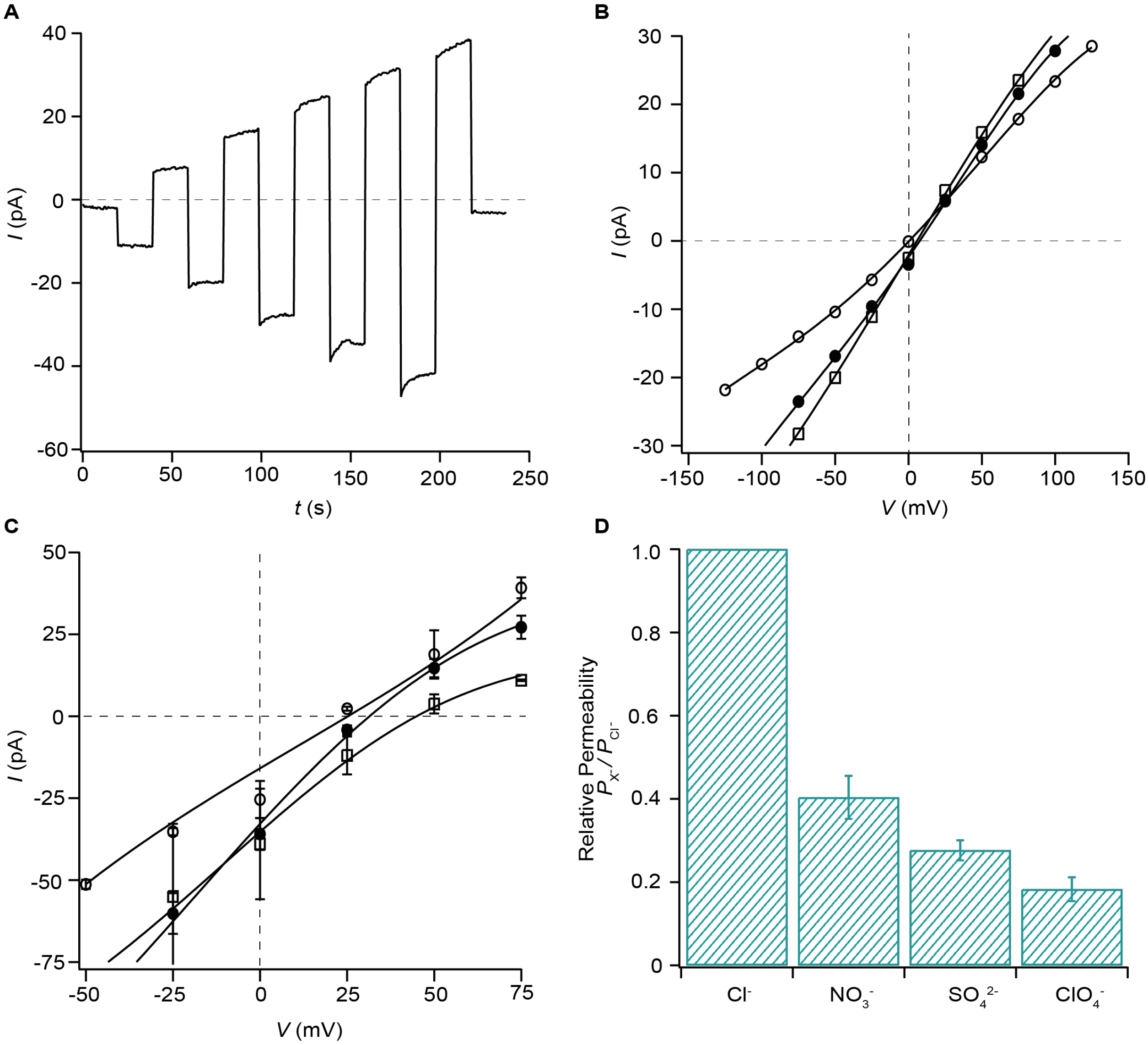

Figure S18. Ion transport characteristics of **2** studied in planar conductance measurements. (A) Current of **2** with 2 M NaCl *cis* and 1 M NaCl *trans* and $V(t)$ = 0 (0), -25 (90), +25 (180), -50 (240), +50 (380), -75 (420), +75 (500), -100 (600), +100 (700), -125 (800), +125 mV (900 s). (B) *I*-*V* profile of **2** with 2 M NaCl *cis* and 2 M (○), 1 M (□) or 0.5 M NaCl *trans* (●). (C) Same with 2 M $NaNO_3$ (○), 2 M $NaClO_4$ (□) or 1 M Na_2SO_4 *trans* (●). (D) Relative ion permeability of **2** normalized by the largest value of the observed ion permeability.

Table S1. Conductance Characteristics of Anion Transporters.

Entry	Cpd[a]	2 M NaCl *cis* : 1 M NaCl *trans*		2 M NaCl *cis* : 0.5 M NaCl *trans*		2 M NaCl *cis* : 2 M $NaNO_3$ *trans*	
		V_r^b (mV)	P_{Cl^-} / P_{Na^+} [c]	V_r^b (mV)	P_{Cl^-} / P_{Na^+} [c]	V_r^b (mV)	P_{NO3^-} / P_{Cl^-} [c]
1	**6**[e]	11.6 ± 0.5	5.0 ± 0.5	19 ± 3	4 ± 1	31 ± 4	0.30 ± 0.04
2	**4**[f]	14.5 ± 0.2	10.4 ± 0.8	25 ± 2	7 ± 1	38.8 ± 0.1	0.22
3	**2**[e]	6.0 ± 0.5	2.1 ± 0.1	9 ± 1	1.8 ± 0.1	23 ± 3	0.40 ± 0.05

Table S1. Continued

Entry	Cpd[a]	2 M NaCl *cis* : 1 M Na_2SO_4 *trans*		2 M NaCl *cis* : 2 M $NaClO_4$ *trans*		z_g^d
		V_r^b (mV)	$P_{SO4^{2-}}$/ P_{Cl^-} [c]	V_r^b (mV)	P_{ClO4^-} / P_{Cl^-} [c]	
1	**6**[e]	40 ± 2	0.21 ± 0.02	41 ± 4	0.21 ± 0.03	0.40 ± 0.08
2	**4**[f]	54.1 ± 0.6	0.12	15 ± 4	0.56 ± 0.08	0.72 ± 0.06
3	**2**[e]	33 ± 2	0.28 ± 0.03	44 ± 4	0.18 ± 0.03	0.39 ± 0.06

[a]Compounds. See Figure 1 and 2 for structures. [b]Reversal potentials V_r which correspond to zero current voltages as determined from the *I-V* profiles (Figures 2, S16, S17, S18). [c]Permeability ratios in planar bilayer conductance from the GHK equation applied to V_r with NaCl (2 M *cis*) and NaCl/NaX gradients in *trans* (where X: NO_3^-, ClO_4^-, SO_4^{2-}). [d]Gating charge as determined by non-linear fitting to equation (S6). [e]Except z_g's (see *d*), reported are mean values ± standard deviations obtained from three independent experiments. [f]Except z_g's (see *d*), reported are mean values ± standard deviations obtained from two independent experiments.

6. Computational Data

6.1. Methods

Calculations were performed using the Gaussian09 program,[S10] all structures were optimized with and without bromide and nitrate using M06-2X/6-311G**. The basis set aug_cc-pVTZ was used for heavy atoms such as Br, Se, Sb, Te, I. For each geometry optimization, frequency calculations were performed to confirm minima (no negative frequencies). Binding energies were compensated for the basis set superposition error (BSSE) with the counterpoise method.[S11]

6.2. Cartesian Coordinates of Nitrate Complexes

Carrier **2**:

C	-0.152585	-2.537198	-0.114773
C	-0.635779	-1.406308	-0.750479
C	-1.712144	-1.603946	-1.591506
C	-2.292968	-2.845787	-1.809785
C	-1.776467	-3.948944	-1.153440
C	-0.696754	-3.799224	-0.297086
Sb	0.195484	0.720101	-0.392303
O	1.489204	2.424483	0.643821
N	0.779905	3.333442	1.225778
O	-0.433321	3.144018	1.334236
F	-2.250714	-0.566705	-2.258951
F	-3.332293	-2.997394	-2.636959
F	-2.314454	-5.155210	-1.345868
F	-0.205830	-4.872318	0.330286
F	0.895132	-2.452886	0.719275
C	-0.092000	0.197403	1.706349
C	-1.397784	0.158299	2.158471
C	-1.730903	-0.096004	3.477747
C	-0.714825	-0.321849	4.390944
C	0.604904	-0.293338	3.975052

C	0.896421	-0.035288	2.643257
F	-2.404786	0.370020	1.297879
F	2.184730	-0.036892	2.297580
F	1.577124	-0.524164	4.860821
F	-1.008075	-0.572270	5.667933
F	-3.003182	-0.125530	3.881463
C	2.171043	-0.041061	-0.881105
C	2.267166	-0.965081	-1.926780
C	3.503241	-1.396297	-2.399905
C	4.672618	-0.906194	-1.831770
C	4.592613	0.023353	-0.800664
C	3.356227	0.459961	-0.333786
H	1.368103	-1.366570	-2.384220
H	1.548532	-2.117959	-3.208406
H	5.638567	-1.243622	-2.191398
H	5.499221	0.416351	-0.353229
H	3.312108	1.192730	0.460134
O	1.340065	4.328545	1.637813

Carrier **4**:

C	-1.097180	0.977045	2.333173
C	-0.142409	0.283200	1.606148
C	0.544688	-0.705394	2.290359
C	0.298682	-1.011731	3.620121
C	-0.674963	-0.307146	4.306736
C	-1.380179	0.694254	3.660845
Te	0.299145	0.684384	-0.521577
O	0.232324	1.170469	-2.883438
N	-0.113760	0.253365	-3.721120
O	-0.734272	-0.725352	-3.305477
F	1.497607	-1.419140	1.675700
F	0.980977	-1.973810	4.247284
F	-0.927649	-0.585946	5.586691
F	-2.310313	1.379719	4.331487

F	-1.797980	1.970607	1.771050
C	-1.781293	0.600943	-0.859597
C	-2.487782	-0.573779	-0.661218
C	-3.839186	-0.669500	-0.948016
C	-4.505369	0.432682	-1.454624
C	-3.821919	1.617808	-1.664043
C	-2.471552	1.692280	-1.360393
F	-1.884308	-1.662636	-0.186807
F	-1.866687	2.859720	-1.554780
F	-4.478688	2.680164	-2.135380
F	-5.807576	0.355597	-1.730775
F	-4.505020	-1.809431	-0.749152
O	0.184631	0.400207	-4.893250

Carrier **6**:

C	0.304881	-0.233631	5.045138
C	0.414877	-1.613006	5.080030
C	0.412745	-2.328334	3.895009
C	0.300524	-1.654492	2.688348
C	0.188723	-0.273479	2.619212
C	0.194004	0.414037	3.824117
F	0.523184	-2.248845	6.248256
F	0.520574	-3.659209	3.929795
F	0.305953	-2.395401	1.578526
I	0.019208	0.742300	0.753382
N	-1.061776	2.204291	-2.012099
F	0.092775	1.744321	3.851521
F	0.308677	0.455717	6.189196
O	-2.095648	1.839273	-1.444765
O	-1.079742	2.792229	-3.087221
O	0.064565	1.962352	-1.46265

Carrier **7**:

C	-1.249271	0.893141	2.353392

C	-0.365449	0.103242	1.642205
C	0.265582	-0.912809	2.337425
C	0.049730	-1.130367	3.688446
C	-0.835191	-0.312263	4.371846
C	-1.494126	0.705965	3.704892
Sb	-0.094152	0.510382	-0.484934
C	2.027387	0.088355	-0.646199
C	2.495277	-0.210094	-1.911039
C	3.835711	-0.382293	-2.198199
C	4.757044	-0.244534	-1.172772
C	4.327485	0.059857	0.106915
C	2.971740	0.227379	0.353601
F	1.616393	-0.360682	-2.914448
F	4.252917	-0.677969	-3.430167
F	6.056495	-0.407478	-1.418857
F	5.223579	0.187318	1.087013
F	2.621508	0.523867	1.605995
F	1.126250	-1.730873	1.720802
F	0.675737	-2.111724	4.340325
F	-1.057866	-0.511732	5.670231
F	-2.356153	1.478921	4.366892
F	-1.924288	1.868539	1.736930
C	-0.611383	-1.741920	-0.722264
C	-1.957277	-2.002039	-0.543158
C	-2.531515	-3.256471	-0.666678
C	-1.715165	-4.326002	-0.993163
C	-0.358882	-4.120174	-1.179999
C	0.163541	-2.841497	-1.040383
F	-2.787026	-0.987812	-0.211309
F	1.489383	-2.731766	-1.218183
F	0.423326	-5.158983	-1.486204
F	-2.231953	-5.548994	-1.123381
F	-3.839402	-3.453187	-0.478923
N	1.203627	3.292200	-0.316258

O	1.487225	4.410377	0.050876
O	1.321268	2.907575	-1.485415

6.3. Cartesian Coordinates of Bromide Complexes

Carrier **4**:

C	0.291976	0.542854	2.874739
C	-0.226405	-0.284263	1.890052
C	-0.318984	-1.637294	2.180708
C	0.099048	-2.158085	3.394781
C	0.606716	-1.308110	4.361206
C	0.702287	0.047412	4.103249
Te	-0.867302	0.502500	0.028343
C	0.653411	-0.922892	-0.945155
C	0.305644	-1.599139	-2.096943
C	1.187445	-2.403745	-2.803986
C	2.482544	-2.552809	-2.341607
C	2.875506	-1.891340	-1.190772
C	1.960274	-1.090115	-0.524140
F	-0.938179	-1.497309	-2.598495
F	2.422005	-0.459478	0.571821
F	4.133895	-2.031133	-0.751341
F	3.352482	-3.322752	-3.007174
F	0.810044	-3.042119	-3.920661
F	-0.814603	-2.502771	1.293310
F	0.005879	-3.467662	3.651159
F	1.006448	-1.797443	5.538155
F	1.209652	0.858059	5.036227
F	0.452890	1.842275	2.664838
Br	-2.870117	2.379773	1.310462

Carrier **6**:

C	0.227830	-0.101996	4.761476
C	0.493225	-1.460555	4.772655

C	0.499588	-2.166037	3.581649
C	0.239697	-1.501218	2.392392
C	-0.029313	-0.143120	2.347503
C	-0.028291	0.534177	3.555846
F	0.741672	-2.086931	5.925680
F	0.756360	-3.477841	3.597026
F	0.259384	-2.233722	1.274680
I	-0.433586	0.876333	0.470551
Br	-0.983461	2.261283	-2.078000
F	-0.277777	1.846176	3.606825
F	0.222698	0.575426	5.913894

6.4. Cartesian Coordinates of Iodide Complexes

Carrier **4**:

C	0.451866	0.479986	2.741296
C	-0.201280	0.312379	1.807750
C	-0.461565	-1.627941	2.151946
C	-0.109986	-2.144327	3.389598
C	0.521984	-1.327322	4.309410
C	0.806751	-0.010772	3.985910
Te	-0.846286	0.475640	-0.039998
C	0.663004	-0.842551	-0.994725
C	0.317342	-1.627928	-2.080016
C	1.221601	-2.458765	-2.723748
C	2.528268	-2.515055	-2.269802
C	2.914219	-1.739332	-1.189170
C	1.981772	-0.914868	-0.579051
F	-0.934572	-1.609725	-2.560408
F	2.417349	-0.168929	0.446075
F	4.179551	-1.789934	-0.763627
F	3.414255	-3.307897	-2.875121
F	0.854932	-3.207298	-3.767908
F	-1.072376	-2.452995	1.298152

F	-0.377429	-3.413883	3.705425
F	0.866468	-1.809693	5.503268
F	1.430806	0.762186	4.875813
F	0.769589	1.738822	2.468185
I	-2.813712	2.029371	1.879522

Carrier **6**:

C	0.496407	-1.470209	4.786749
C	0.501863	-2.175273	3.595389
C	0.242101	-1.510125	2.406491
C	-0.025626	-0.151807	2.365220
C	-0.024142	0.52659	3.572762
C	0.232063	-0.111341	4.777233
F	0.757408	-3.486819	3.608465
F	0.260331	-2.239717	1.288192
I	-0.428470	0.865516	0.496079
F	-0.272675	1.837669	3.622954
F	0.227648	0.565876	5.929186
F	0.744720	-2.097323	5.938656
I	-1.023601	2.368934	-2.265200

7. References

(S1) Benz, S.; Poblador-Bahamonde, A. I; Low-Ders, N.; Matile, S. Catalysis with Pnictogen, Chalcogen and Halogen Bonds. *Angew. Chem. Int. Ed.* **2018**, *57*, 5408-5412.

(S2) Kemmitt, R.D.; Nichols, D. I.; Peacock, R.D. Preparation and Reaction of Tris(pentafluorophenyl)phosphine, Phenylbis(pentafluorophenyl)phosphine, and Diphenylpentafluorophenylphophine complexes of Rhodium. *J. Chem Soc. A* **1968**, 2149-2152.

(S3) Tyrra, W. E. Oxidative Perfluoroorganylation Methods in Group 12-16 chemistry: the Reactions of Haloperfluoroorgnics and In and InBr, a Convenient New Route to AgR_f(R_f= CF_3, C6F5) and Reaction of AgR_f with group 12-16 Elements. *J. Fluor. Chem.* **2001**, *112*, 149-152.

(S4) Benz, S.; Macchione, M.; Verolet, Q.; Mareda, J.; Sakai, N.; Matile, S. Anion Transport with Chalcogen Bonds. *J. Am. Chem. Soc.* **2016**, *138*, 9093-9096.

(S5) Vargas-Jentzsch, A.; Emery, D.; Mareda, J.; Nayak, S. K.; Metrangolo, P.; Resnati, G.; Sakai, N.; Matile, S. Transmembrane Anion Transport Mediated by Halogen-Bond Donors. *Nat. Commun.* **2012**, *3*, 905.

(S6) Macchione, M.; Tsemperouli, M.; Goujon, A.; Mallia, A. R.; Sakai, N.; Sugihara, K.; Matile, S. Mechanosensitive Oligodithienothiophenes: Transmembrane Anion Transport Along Chalcogen-Bonding Cascades. *Helv. Chim. Acta* **2018**, *101*, e1800014.

(S7) Perez-Velasco, A.; Gorteau, V.; Matile, S. Rigid Oligoperylenediimide Rods: Anion-π Slides with Photosynthetic Activity. *Angew. Chem. Int. Ed.* **2008**, *47*, 921-923.

(S8) Tsemperouli, M.; Sugihara, K. Characterization of di-ANEPPS with Nano-Black Lipid Membranes. *Nanoscale* **2018**, *10*, 1090-1098.

(S9) (a) Jin, T. Selective Transport of Potassium Ions Across a Planar Phospholipid Bilayer by a Calix[4]arene-crown-5 as a Synthetic Carrier. *J. Am. Chem. Soc.* **2002**, *1*, 151-154. (b) Sakai, N.; Houdebert, D.; Matile, S. Voltage-Dependent Formation of Anion Channels by Synthetic Rigid-Rod Push-Pull β-Barrels. *Chem. Eur. J.* **2003**, *9*, 223-232.

(S10) Frisch, M. J.; Trucks, G. W.; Schlegel, H. B.; Scuseria, G. E.; Robb, M. A.; Cheeseman, J. R.; Scalmani, J. R.; Barone, V.; Mennucci, B.; Petersson, G. A.; Naktsuji, H.; Caricato, M.; Li, X.; Hratchian, H. P.; Izmylov, A. F.; Bloino, J.; Zheng, G.; Sonnenberg, J. L.; Hada, M.; Ehara, M.; Toyota, K.; Fukuda, R.; Hasegawa, J.; Ishida, M; Nkajim, T.; Honda, Y.; Kitao, O.; Nakai, H.; Vreven, T.; Montgomery Jr., J. A.; Peralta, J. E.; Ogliaro, F.; Bearpark, M.; Heyd, J.: Brothers, E.; Kudin, N.; Staroverov, V. N.; Kobayashi, R.; Normnd, J.; Raghavachari, K.; Rendell, A.; Burant, J. C.; Iyengar, S. S.; Tomasi, J.; Cossi, M.; Rega, N.; Millam, J. M.; Klene, M.; Knox, J. E.; Cross, J. B.; Bakken, V.; Adamo, C.; Jaramillo, J.; Gomperts, R.; Stratmann, R. E.; Yazyev, O.; Austin, A. J.; Cammi, R.; Pomelli, C.; Ochterski, J. W.; Martin, R. L.; Morokuma, K.; Zakrzewski, V. G.; Voth, G. A.; Salvador, P.; Dannenberg, J. J.; Dapprich, S.; Daniels, A. D.; Farkas, Ö.; Foresman, J. B.; Ortiz, J. V.; Cioslowski, J.; Fox, D. J. *Gaussian 09*, Revision D.01; Gaussian Inc.: Wallingford CT, 2009.

(S11) Boys, S. F.; Bernardi, F. The Calculation of Small Molecular Interactions by the Differences of Separate Total Energies. Some procedures with Reduced Errors. *Mol. Phys*. **1970**, *19*, 553-566.